Table VI—Theoretical Proton Ratios for Various Protons Involved in Polymeric Alcohols Containing Various Numbers of Trioxane Rings

Protons	Proton Ratios (Group per OH)			
	1 Ring	2 Rings	3 Rings	4 Rings
Ring CH	1.0	1.5	1.8	2.0
Aliphatic CH_2	12.0	15.0	16.8	18.0
Methyl	12.0	15.0	16.8	18.0

The ratio of various protons having different chemical shifts would be expected to vary as polymerization continued. In particular, the ratio of ring CH, aliphatic CH_2, and methyl protons to hydroxyl protons would increase as the number of bridged trioxane rings increased (Table VI).

While it was important to separate individual components for characterization, this need does not apply for the establishment of drug purity. The gel permeation technique was modified to allow analysis of the total polymeric material in drug samples. To validate this method of analysis, mixtures having known compositions were analyzed. The results (percent impurity added: 0, 5.2, and 9.4; found: 0, 5.1, and 9.4) indicate that the method described under *Experimental* is sufficiently accurate for use.

CONCLUSIONS

Available information indicates that contaminants present in certain batches of I consist of polymeric alcohols characterized by at least one trioxane ring. These contaminants originate in the dialdehyde precursor, which may polymerize to form corresponding compounds. Reduction of polymers present in the dialdehyde yields the alcohol polymers, which may persist throughout purification and contaminate the finished drug. Analysis *via* gel permeation liquid chromatography provides a useful means to analyze the degree of contamination by these polymeric compounds.

REFERENCES

(1) H. P. Blumenthal, J. R. Ryan, and F. G. McMahon, *Clin. Pharmacol. Ther.*, **17**, 229 (1975).

(2) O. P. Goel, *Chem. Ind. (London)*, **16**, 665 (1974).

(3) J. L. Mulder and F. A. Buytenhuys, *J. Chromatogr.*, **51**, 459 (1970).

(4) *Thermal Analysis Newsletter*, vols. 5 and 6, Perkin-Elmer Corp., Norwalk, Conn.

(5) J. March, "Advanced Organic Chemistry: Reactions, Mechanisms, and Structure," McGraw-Hill, New York, N.Y., 1968, p. 717.

(6) J. D. Roberts and M. C. Caserio, "Basic Principles of Organic Chemistry," W. A. Benjamin, New York, N.Y., 1965, pp. 448, 449.

(7) J. C. Bevington, *Q. Rev. (London)*, **6**, 141 (1952).

(8) M. Baron, D. B. Mandirola, and J. F. Westerkamp, *Can. J. Chem.*, **41**, 1893 (1963).

(9) K. Rast, *Chem. Ber.*, **55**, 1051, 3727 (1922).

ACKNOWLEDGMENTS

The authors are indebted to Dr. O. Goel, who synthesized most of the materials used in this study, to Mr. B. Scott, who determined the NMR spectra, and to Dr. L. M. Wheeler for encouragement and support.

Preliminary Model for Streptozocin Metabolism in Mice

JONAS M. WEISSBROD * and RAKESH K. JAIN ‡x

Received June 25, 1979, from the **Department of Chemical Engineering, Columbia University, New York, NY 10027*, and the ‡*Department of Chemical Engineering, Carnegie-Mellon University, Pittsburgh, PA 15213.* Accepted for publication January 18, 1980.

Abstract □ A mathematical model for streptozocin metabolism in mice is presented. By using the available bioassay and chemical assay data for a 300-mg/kg ip injection and the principles of physiologically based pharmacokinetics, a membrane-limited transport model with first-order kinetics was found to simulate the data adequately (average error of <20%). Furthermore, the first-order reaction constant derived in analyzing the bioassay data (0.009 min^{-1}) was in close agreement with the half-life of streptozocin (1 hr) reported previously.

Keyphrases □ Streptozocin—drug metabolism and distribution, mathematical model based on bioassay and chemical assay, mice □ Metabolism—streptozocin distribution and transport, mice, mathematical model □ Diabetes—streptozocin induced, pharmacokinetic model, mice □ Pharmacokinetic models—streptozocin metabolism, bioassay and chemical assay, mice, membrane-limited transport

Streptozocin (NSC-85998), the 2-deoxy-D-glucose derivative of 1-methylnitrosourea (1), has been shown to inhibit primary DNA synthesis in mammalian cells (2, 3). Due to its selective toxicity for pancreatic β-cells, streptozocin has been used to induce diabetes in a variety of animals (4–6). In addition, it has been useful in the treatment of metastatic insulinoma (7, 8).

BACKGROUND

Previous kinetic studies showed that streptozocin degradation obeys first-order reaction kinetics. These studies also indicated the presence of at least two pathways for streptozocin degradation, one involving the *N*-nitroso group and the other involving another portion of the molecule, probably the glucose moiety (9). While chromatography has been used to isolate several streptozocin metabolites (10, 11), their molecular structures have not been identified precisely.

In addition, data for streptozocin concentrations in various tissues of mice as a function of time were obtained previously (10) using three assay methods: bioassay and chemical and radiochemical assays. The bioassay is the closest indicator of the actual streptozocin content, but this method does not preclude the possibility that some drug metabolites also may be bioactive. The chemical assay measures the *N*-nitroso group of streptozocin and its metabolites. The radiochemical assay measures a tritiated hydrogen atom that originally was at the C-6 position of the glucose moiety of streptozocin and must be accounted for either as part of the streptozocin molecule or as part of the several streptozocin metabolites known to exist.

The objective of this study was to utilize these data along with the present knowledge of streptozocin metabolism to develop mathematical models for the distribution, transport, and metabolism of streptozocin in mice.

THEORETICAL

In recent years, physiologically based pharmacokinetic modeling (12, 13) has been applied extensively to predict drug distributions in plasma and various tissues of mammalian systems (14, 15). A pharmacokinetic model is a simplified representation of a real physical system (Scheme I) derived from experimental observations, previous knowledge, and a number of assumptions. It is based on relevant physical and biochemical parameters such as plasma flow rates, tissue volumes, tissue binding constants, mass transfer coefficients, and, when necessary, chemical reaction constants to account for drug metabolism. The validity of the model as a means of predicting tissue drug distributions and excretion rates is tested by comparing model predictions with data. Plasma flow rates and tissue volumes for most species and tissues are readily available in the literature. Mass transfer, binding, and metabolism parameters for a given drug must be estimated from the available data.

0022-3549/80/0600-0691$01.00/0

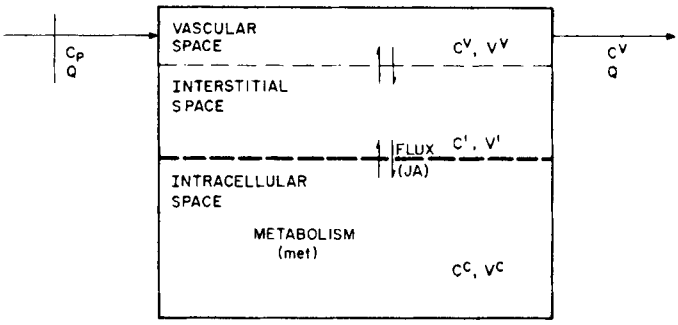

Scheme I—Schematic representation of a typical model compartment where Q is the plasma perfusion rate; C_p is the afferent plasma concentration; V^v, V^i, and V^c are the volumes of the vascular, interstitial, and intracellular spaces, respectively; C^v, C^i, and C^c are the drug concentrations in the vascular, interstitial, and intracellular spaces, respectively; jA is the net flux of drug to the intracellular space; and met is the rate of drug disappearance via metabolism. The vascular and interstitial spaces are combined into a single extracellular subcompartment, and the efferent plasma concentration is assumed to be equal to the extracellular drug concentration.

As shown in Scheme I, a tissue compartment can be divided into three subcompartments: the vascular, interstitial, and intracellular spaces. Drug concentrations in each subcompartment are assumed to be uniform, and the effluent plasma concentration is assumed to be equal to the drug concentration of the vascular subcompartment.

For most drugs and tissues, the vessel wall is more permeable than the cellular membrane, and the vascular and interstitial subcompartments can be combined into a single subcompartment, the extracellular space. Therefore, in the present study, transport in all of the compartments was modeled according to a membrane-limited model, which is similar to models applied previously to methotrexate uptake into the bone marrow, spleen, and intestine of rats (13), dactinomycin (actinomycin D) uptake into the testes of beagle dogs (16), and methotrexate uptake into several types of tumors (17, 18).

With these assumptions and definitions, two nonsteady-state material balance equations for a particular body (or tissue) compartment may be derived:

$$V_i^e \frac{dC_i^e}{dt} = Q_i(C_p - C_i^e) - (jA)_i - q_i C_i^e \qquad \text{(Eq. 1)}$$

$$V_i^c \frac{dC_i^c}{dt} = (jA)_i - (\text{met})_i \qquad \text{(Eq. 2)}$$

where the subscript i refers to the ith body compartment; V_i^e and V_i^c are the volumes of the extracellular and intracellular spaces (milliliters), respectively; C_i^e and C_i^c are the total drug concentrations in the extracellular and intracellular spaces (micrograms per milliliter), respectively; Q_i is the plasma perfusion rate (milliliters per minute); q_i is the drug clearance rate (zero for compartments other than the kidneys and liver) that accounts for drug elimination *via* the urine and bile (milliliters per minute); C_p is the afferent plasma concentration (micrograms per milliliter); $(jA)_i$ is the net flux of drug into the intracellular subcompartment (micrograms per minute); and $(\text{met})_i$ is the rate of drug metabolism in the ith compartment (micrograms per minute).

The net flux $(jA)_i$ between the extracellular and intracellular subcompartments and the relationship between free and bound drug are defined by:

$$(jA)_i = V_i h_i (C_i^e - C_i^c/R_i) \qquad \text{(Eq. 3)}$$

where h_i and R_i are apparent first-order diffusion constants and tissue equilibrium partition coefficients into which the effect of drug binding in the extracellular fluid has been incorporated, respectively. The use of a first-order diffusion constant, h_i, assumes that the transport mechanism across the cell membrane is linear and nonsaturable.

The drug metabolism rate, $(\text{met})_i$, in the intracellular subcompartment is defined by:

$$(\text{met})_i = k_i V_i C_i^c \qquad \text{(Eq. 4)}$$

where k_i is the first-order reaction constant for streptozocin degradation. The use of first-order kinetics to describe streptozocin degradation was verified by previous kinetic studies (9).

Previous pharmacokinetic studies illustrated the applicability of a nonlinear regression analysis to the available plasma data to obtain an exponential equation for plasma concentrations as a function of time (15, 17, 18). This approach was utilized in the present study. Thus, once the parameter values and plasma exponential equations are known, Eqs. 1 and 2 are solved to obtain predictions for streptozocin concentrations in a given tissue as a function of time.

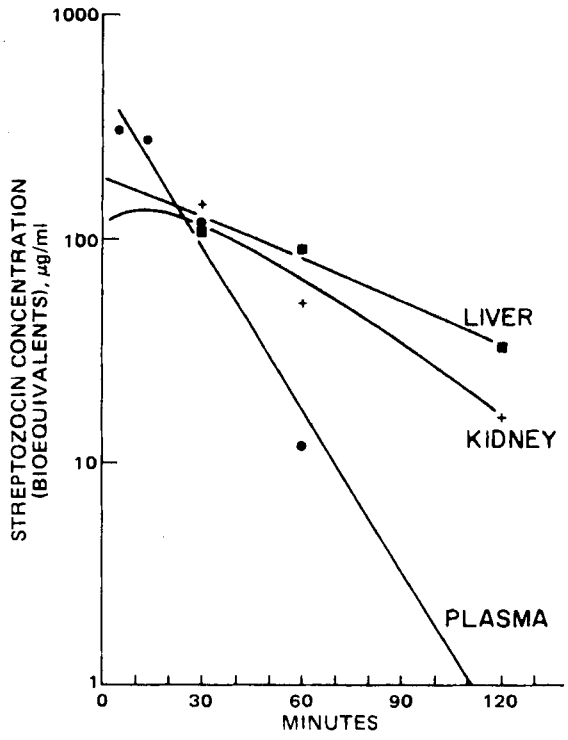

Figure 1—*Streptozocin bioequivalents* versus *time in plasma, liver, and kidneys of mice following an injection of 300 mg/kg ip. Points represent the experimental data of Bhuyan* et al. *(10) for plasma (●), liver (■); and kidneys (+). The curves represent model predictions. The parameters of Table I (bioassay values) and an exponential equation for the plasma concentration ($494.53e^{-0.0549t}$) were used to obtain the simulations.*

To compare model predictions with the data, the average drug concentration in a tissue must be defined as:

$$C_i = (C_i^e V_i^e + C_i^c V_i^c)/V_i \qquad \text{(Eq. 5)}$$

where C_i is the overall drug concentration of the ith compartment (micrograms per milliliter).

EXPERIMENTAL

Data for streptozocin concentrations as a function of time were obtained by Bhuyan *et al.* (10) using three independent assay methods: bioassay, chemical assay, and radiochemical assay. In these experiments, streptozocin (tritiated or unlabeled) was dissolved in phosphate buffer and was administered intraperitoneally to 20-g female BDF_1 (C57BL/6 × DBA/2) mice[1]. At various postinjection times up to 2 hr, groups of mice (four or five per group) were sacrificed; blood samples were collected, tissues were excised, and all were assayed for streptozocin.

The experimental procedures used were those described by Bhuyan *et al.* (10).

RESULTS AND DISCUSSION

Values for the compartmental volumes and tissue flow rates (V_i and Q_i, respectively) for each tissue were obtained from the literature (19). The binding, diffusion, and metabolism constants (R_i, h_i, and k_i) were determined by applying parameter estimation methods (18, 20) to the data of Bhuyan *et al.* (10). With these parameter values (Table I), the chemical and bioassay data for the liver, kidneys, and pancreas were modeled by first obtaining exponential fits for the plasma data and then solving Eqs. 1 and 2 for each tissue. The results are shown in Figs. 1 and

[1] Jackson Memorial Laboratory, Bal Harbor, Me.

Table I—Model Parameters [a] for Streptozocin Distribution in Mice [b]

Tissue	Tissue Volume (V), ml	Extracellular Volume (V^e), ml[d]	Plasma Flow Rate (Q), ml/min	Partition[c] Coefficient (R) Bio	Partition[c] Coefficient (R) Chem	Diffusion Constant[c] (h), min^{-1} Bio	Diffusion Constant[c] (h), min^{-1} Chem	Reaction Constant[c] (k), min^{-1} Bio	Reaction Constant[c] (k), min^{-1} Chem
Liver[e]	1.30[f]	0.5	1.1[f]	23.6	19.7	0.0164	0.1392	0.0086	0.0041
Kidneys[g]	0.34	0.13	0.8[f]	5.6	7.7	0.0305	0.1625	0.0096	0.0041[h]
Pancreas	0.09[b]	0.04	0.048[b]	—	15.8	—	0.0063	—	0.0041[h]

[a] Data were obtained by bioassay and chemical assay methods. [b] Mice weighed 20 g. [c] Obtained by parameter estimation using the bioassay and chemical assay data of Bhuyan *et al.* (10) for an injection of 300 mg/kg ip. [d] Estimated. [e] Bile clearance, q_1, is negligible (10). [f] Taken from Ref. 19. [g] Kidney clearance, q_k, was estimated from the data of Bhuyan *et al.* (10) to be 0.42 ml/min. [h] Assumed.

2. The average error between the data and the model predictions was 18.3% for the bioassay data (Fig. 1) and 15.1% for the chemical assay data (Fig. 2). The model also was applied to obtain fits for the radiochemical assay data (20). Since the parameter values obtained from the radioassay data are of limited value because of the rapid metabolism of streptozocin, these results are not given here.

The models presented in this report utilize data for an intraperitoneal injection of 300 mg/kg. They also provide a quantitative basis for the prediction of drug distributions at other doses and for other modes of injection. Such extensions were discussed previously for other drugs (16–18). In addition, the development of membrane-limited models for drug transport and the inclusion of terms to account for tissue binding and drug metabolism are emphasized here.

The bioassay is the best available measure of the whole streptozocin molecule. In modeling the bioassay data, a reaction constant of ~0.009 min^{-1} was determined for both the kidneys and the liver. This value is in good agreement with a half-life of ~1 hr, which was reported previously (9).

As stated previously, the chemical assay is a measure of the *N*-nitroso group of streptozocin and its metabolites. Previous investigators related the mode of action of streptozocin and other nitrosoureas to the alkylation of various cell components (*i.e.*, DNA, RNA, nucleic acid precursors, and proteins) and the subsequent inhibition of cell division and other critical biochemical processes (21, 22). The observed suppression of NAD^+ and inhibition of pyridine synthesis (23–27) also may be explained within the context of this mode of action.

The degradation pattern of streptozocin to yield a methyl carbonium ion capable of alkylating various cell constituents can be envisioned as a two-step process with methyldiazonium ion as an intermediate. This process is consistent with the known biological degradation patterns for *N*-nitrosoureido compounds (28) and illustrates the importance of the chemical assay in measuring drug activity relative to the proposed mode of drug action.

While the present analysis describes the available data in mice adequately, more data are needed to characterize the transport and metabolism more precisely. Chromatography has isolated several streptozocin metabolites (10, 11), but further work is needed for their identification. As those findings become available, they can be incorporated into a more complex pharmacokinetic model to describe the drug metabolism. In addition, detailed drug distribution data at different dose levels and for different species should be collected and compared with the present pharmacokinetic model as has been done for other drugs (14). Finally, pharmacokinetic studies on other nitrosoureas and glucose-like drugs would provide quantitative information about their transport, mode of action, and metabolism and additional insights into streptozocin pharmacokinetics.

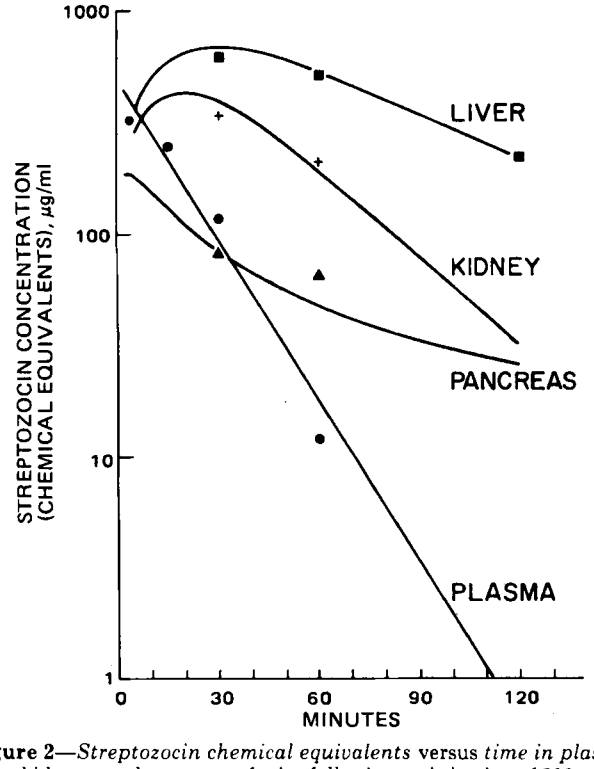

Figure 2—*Streptozocin chemical equivalents* versus *time in plasma, liver, kidneys, and pancreas of mice following an injection of 300 mg/kg ip. Points represent the experimental data of Bhuyan* et al. *(10) for plasma (●), liver (■), kidneys (+), and pancreas (▲). The curves represent model predictions. The parameters from Table I (chemical assay values) and an exponential equation for the plasma concentration ($494.53e^{-0.0549t}$) were used to obtain the simulations.*

REFERENCES

(1) R. R. Herr, J. K. Jahnke, and A. D. Argoudelis, *J. Am. Chem. Soc.*, **89**, 4808 (1967).

(2) B. K. Bhuyan, *Cancer Res.*, **30**, 2017 (1970).

(3) F. R. Reusser, *J. Bacteriol.*, **105**, 580 (1971).

(4) N. Rakienten, M. L. Rakienten, and M. V. Nadkarni, *Cancer Chemother. Rep.*, **29**, 91 (1963).

(5) J. S. Evans, G. C. Gerritsen, K. M. Mann, and S. P. Owen, *ibid.*, **48**, 1 (1965).

(6) A. Junod, A. E. Lambert, L. Orci, R. Pictet, A. E. Gonet, and A. E. Renold, *Proc. Soc. Exp. Biol. Med.*, **126**, 201 (1967).

(7) I. M. Murray-Lyon, A. L. Eddleston, R. Williams, M. Brown, B. M. Hogbin, A. Bennett, J. C. Edwards, and K. W. Taylor, *Lancet*, **2**, 895 (1968).

(8) L. E. Broder and S. K. Carter, *Ann. Intern. Med.*, **79**, 108 (1973).

(9) E. R. Garrett, *J. Am. Pharm. Assoc., Sci. Ed.*, **49**, 767 (1960).

(10) B. K. Bhuyan, S. L. Kuentzel, L. G. Gray, T. J. Fraser, D. Wallach, and G. L. Neil, *Cancer Chemother. Rep.*, **58**, 157 (1974).

(11) E. H. Karunanayake, D. J. Hearse, and G. Mellows, *Biochem. J.*, **142**, 673 (1974).

(12) R. L. Dedrick and K. B. Bischoff, *Chem. Eng. Prog. Symp. Ser.*, **64**, 32 (1968).

(13) R. L. Dedrick, D. S. Zaharko, and R. J. Lutz, *J. Pharm. Sci.*, **62**, 882 (1973).

(14) K. J. Himmelstein and R. J. Lutz, *J. Pharmacokinet. Biopharm.*, **7**, 127 (1979).

(15) R. K. Jain, J. Wei, and P. M. Gullino, *ibid.*, **7**, 181 (1979).

(16) R. J. Lutz, W. M. Galbraith, R. L. Dedrick, R. Shrager, and L. B. Mellett, *J. Pharmacol. Exp. Ther.*, **200**, 469 (1977).

(17) R. J. Lutz, R. L. Dedrick, J. A. Straw, M. M. Hart, P. Klubes, and D. S. Zaharko, *J. Pharmacokinet. Biopharm.*, **3**, 77 (1975).

(18) J. M. Weissbrod, R. K. Jain, and F. M. Sirotnak, *ibid.*, **6**, 487 (1978).

(19) K. B. Bischoff, R. L. Dedrick, D. S. Zaharko, and J. A. Longstreth, *J. Pharm. Sci.*, **60**, 1128 (1971).

(20) J. M. Weissbrod, D. E. S. dissertation, Columbia University, New York, N.Y., 1979 (obtainable from University Microfilms, Ann Arbor, Mich.).

(21) P. N. Magee and J. M. Barnes, *Adv. Cancer Res.*, **10**, 163 (1967).
(22) P. D. Lawley and S. A. Shah, *Biochem. J.*, **128**, 117 (1972).
(23) P. S. Schein and S. Loftus, *Cancer Res.*, **28**, 1501 (1968).
(24) P. S. Schein, D. A. Cooney, M. G. McMenamin, and T. Anderson, *Biochem. Pharmacol.*, **22**, 2625 (1973).
(25) S. S. Lazarus and S. H. Shapiro, *Diabetes*, **22**, 499 (1973).
(26) A. Junod, A. E. Lambert, W. Stauffacher, and A. E. Renold, *J. Clin. Invest.*, **48**, 2129 (1969).
(27) C. K. Ho and S. A. Hashim, *Diabetes*, **21**, 789 (1972).
(28) P. D. Lawley, *Nature*, **218**, 580 (1968).

ACKNOWLEDGMENTS

Supported in part by a grant from the National Science Foundation.

The authors thank Dr. B. K. Bhuyan and Dr. G. L. Neil of The Upjohn Co., Kalamazoo, Mich., for providing information about their data. They also are grateful to Mr. Charles Maldarelli and Mr. Walter Bartynski who participated in the early phase of this work.

Antihyperlipidemic Activity of Sesquiterpene Lactones and Related Compounds

I. H. HALL *x, K. H. LEE *, C. O. STARNES *, O. MURAOKA *, Y. SUMIDA *, and T. G. WADDELL ‡

Received September 28, 1979, from the **Division of Medicinal Chemistry, School of Pharmacy, University of North Carolina, Chapel Hill, NC 27514*, and the ‡*Department of Chemistry, University of Tennessee at Chattanooga, Chattanooga, TN 37401.* Accepted for publication January 23, 1980.

Abstract □ Some naturally occurring pseudoguaianolides and germacranolides as well as synthetic related compounds were observed to be antihyperlipidemic agents in mice. Several of these compounds at a dose of 20 mg/kg/day resulted in lowering of serum cholesterol by ~30% and of serum triglycerides by ~25%. Thiol-bearing enzymes of lipid synthesis, *i.e.*, acetyl-CoA, citrate-lyase, acetyl-CoA synthetase, and β-hydroxy-β-methylglutaryl-CoA reductase, were inhibited by these agents *in vitro*, supporting the premise that these agents alkylate thiol nucleophiles by a Michael-type addition. The α-methylene-γ-lactone moiety, the β-unsubstituted cyclopentenone ring, and the α-epoxycyclopentanone system of these compounds appeared to be responsible for the lowering of serum lipids.

Keyphrases □ Lactones, sesquiterpene—antihyperlipidemic activity, structure–activity relationships, serum levels of cholesterol and triglycerides, mice □ Structure–activity relationships—sesquiterpene lactones, antihyperlipidemic activity, effect on serum levels of cholesterol and triglycerides, mice □ Antihyperlipidemic activity—sesquiterpene lactones, structure–activity relationships, serum levels of cholesterol and triglycerides, mice

Pseudoguaianolide (I, III, IV, V, X, and XI) and germacranolide (XII and XIII) sesquiterpene lactones and related compounds (XIV and XV) are potent antineoplastic agents, effective against Walker 256 carcinosarcoma, Lewis lung carcinoma, P-388 lymphocytic leukemia, and Ehrlich ascites carcinoma in rodents (1). Furthermore, these agents significantly inhibited induced inflammation and arthritic states in rats (2).

In a study of the effects of sesquiterpene lactones on cellular metabolism as antineoplastics, these agents inhibited β-hydroxy-β-methylglutaryl-CoA reductase activity of 10-day-old Ehrlich ascites tumor cells. For example, helenalin (I) at 7 μmoles caused 67% inhibition. Compound I also lowered the elevated serum cholesterol level of tumor-bearing mice by 39% (3). These observations suggested that the sesquiterpene lactones should be tested as antihyperlipidemic agents.

EXPERIMENTAL

Source of Test Compounds—Some of the test compounds are natural products and were isolated from plant species by literature techniques (4). Helenalin (I) was isolated from *Balduina angustifolia*[1] (5); tenulin (V) (6) and aromaticin (XI) (6, 7) were isolated from *Helenium amarum*[2]; deoxyelephantopin (XII) was obtained from *Elephantopus carolinianus*[3] (8); and eupahyssopin (XIII) was isolated from *Eupatorium hyssopifolium*[4] (9).

Plenolin (III) was obtained by hydrogenation of helenalin to give the identical compound as the naturally occurring product (10). 2,3-Dihydrohelenalin (II) and 2,3-epoxyhelenalin (IV) were chemically modified from helenalin (11). Dihydrotenulin (VI), 2,3-epoxytenulin (VII), isotenulin (VIII), 2,3-epoxyisotenulin (X), and dihydroisotenulin (IX) were prepared by the methods of Waddell *et al.* (11). Thymine α-methylene-γ-lactone (XIV) (12), α-methylene-γ-lactone (XVIII) (13), and 2,3-epoxycyclopentan-1-one (XVI) (14) were prepared by literature methods. 2-Cyclopentenone[5] (XV), maleic anhydride[5] (XVII), clofibrate[6] (XIX), and acetazolamide[7] (XX) were obtained commercially.

Serum Hypolipidemic Activity—CF_1 male mice (~30 g) were fed food[8] with water *ad libitum* for the duration of the experiment. The drugs were suspended in 1% carboxymethylcellulose–water and homogenized. The doses were based on the weekly weights of the mice (15). The compounds were tested at 20 mg/kg/day ip.

On Days 9 and 16, blood was collected by tail vein bleeding in alkali-free nonheparinized microcapillary tubes, which then were centrifuged 3 min to obtain the serum. Duplicate 30-μl samples of nonhemolyzed serum were used to determine the serum cholesterol levels in milligram percent by a modification of the Liebermann–Burchard reaction (16). A separate group of mice were bled on Day 14, and their serum triglyceride levels (milligram percent) were determined using duplicate 25-μl samples (17).

Enzymatic Assays—Compounds were tested *in vitro* at 1 μmole for their effects on the enzymatic activity of a 10% liver homogenate prepared in 0.25 *M* sucrose and 0.001 *M* ethylenediaminetetraacetic acid at pH 7.2. Adenosine triphosphate citrate-lyase activity was measured by the method of Hoffmann *et al.* (18). Acetyl-CoA synthetase activity was determined by the method of Goodridge (19). The acetyl-CoA formed

[1] Obtained from Dr. M. E. Wall and H. L. Taylor, Research Triangle Institute, N.C. (No. R.T. 4147); Dr. R. E. Perdue, Jr., U.S. Department of Agriculture, Beltsville, Md., provided the identification number NO PR8878.
[2] Identified by Dr. G. S. Van Horn, Department of Biology, University of Tennessee at Chattanooga, Chattanooga, Tenn. Voucher specimen CAM-81775-FAR-TW is available from Dr. T. G. Waddell for inspection.
[3] Identified by S. W. Leonard, Coastal Zone Resources Corp., Wilmington, N.C. A voucher specimen has been placed in the herbarium of the Department of Botany, University of North Carolina at Chapel Hill, Chapel Hill, N.C.
[4] Obtained from Dr. M. E. Wall and H. L. Taylor, Research Triangle Institute, N.C. Voucher specimen NO PR21478 is available.
[5] Aldrich Chemical Co.
[6] Ayerst Laboratories.
[7] Sigma Chemical Co.
[8] Rodent lab chow, Wayne Blox.

0022-3549/80/0600-0694$01.00/0